



## Fabrication of biodegradable synthetic perfusable vascular networks via a combination of electrospinning and robocasting

Journal:	<i>Biomaterials Science</i>
Manuscript ID:	BM-COM-12-2014-000418
Article Type:	Communication
Date Submitted by the Author:	04-Dec-2014
Complete List of Authors:	Ortega, Ilida; The University of Sheffield, The School of Clinical Dentistry Dew, Lindsey; University of Sheffield, Engineering Materials Department Kelly, Adam; University of Sheffield, Chong, Chuh Khiun; University of Sheffield, Material Science and Engineering MacNeil, Sheila; University of Sheffield, Engineering Materials Department Claeyssens, Frederik; University of Sheffield, Engineering Materials Department

## COMMUNICATION

## Fabrication of biodegradable synthetic perfusable vascular networks via a combination of electrospinning and robocasting

Cite this: DOI: 10.1039/x0xx00000x

Received 00th January 2012,  
Accepted 00th January 2012

Ilida Ortega,<sup>a##</sup> Lindsey Dew,<sup>b#</sup> Adam G. Kelly,<sup>b</sup> Chuh K. Chong,<sup>b</sup> Sheila MacNeil,<sup>b</sup> Frederik Claeysens<sup>b\*</sup>

DOI: 10.1039/x0xx00000x

[www.rsc.org/](http://www.rsc.org/)

**Biodegradable synthetic vascular networks are produced via the combination of robocasting and electrospinning techniques. Preliminary revascularization studies using microvascular endothelial cells and human dermal fibroblasts show good attachment and uniform distribution within the vascular networks, highlighting their potential use in vascular tissue engineering applications.**

One of the greatest challenges currently faced in Tissue Engineering (TE) is the incorporation of vascular networks within tissue engineered constructs. Many of these 3D constructs recapitulate the gross morphology of the native tissues but do not contain any intrinsic vasculature requiring ingrowth of neovasculature from the host wound bed for their survival. When this occurs too slowly TE grafts fail as tissues lack access to oxygen and nutrients. Generally, TE grafts thicker than 400  $\mu\text{m}$  will need the presence of vasculature for avoiding necrosis and allowing diffusion of nutrients and gases<sup>1-3</sup>. The formation of blood vessels in the absence of intrinsic vasculature (vasculogenesis) and in the presence of pre-existing vessels (angiogenesis) has been addressed by tissue engineers using a range of approaches<sup>4</sup>. Many approaches are based on the use of decellularised tissues<sup>5-10</sup> whilst others focus on the use of natural polymers such as collagen<sup>11</sup>. Both natural and synthetic extracellular matrix (ECM) materials have also been used for the creation of patterned vascular networks using carbohydrate-based sacrificial materials<sup>12</sup>. For electrospun constructs, Centola and coworkers reported work on the fabrication of an electrospun hybrid vascular graft reinforced with a PCL frame created by fused deposition modelling<sup>13</sup> and Jeffries and coworkers have recently combined fused deposition modelling with template electrospinning<sup>14</sup>. Furthermore, 3D aortic valve conduits have been produced by Duan et al. using bioprinting methods and an alginate/gelatin hydrogel<sup>15</sup>.

In this study we developed a 4-step technique combining electrospinning and robocasting which allows the introduction of complexity within biodegradable membranes using a cell-friendly sacrificial template material (alginate) as illustrated in Figure 1. This method is very versatile and allows the creation of vascular networks with a wide range of morphologies and sizes as well as the use of a variety of medical grade polymers for the creation of the

biodegradable membranes. Specifically, in this study we used Poly (lactic-co-glycolic acid) (PLGA) and poly (3-hydroxybutyrate-co-3-hydroxyvalerate) (PHBV) for the creation of electrospun mats equipped with artificial vasculature and we used both human dermal fibroblasts (HDFs) and human dermal microvascular endothelial cells (HDMECs) for preliminary cell studies.

Combining conventional techniques routinely used in tissue engineering approaches such as electrospinning and innovative 3D additive manufacturing techniques such as robocasting brings numerous advantages to the design of future medical devices. Some of these advantages have been previously reported by our groups in several publications highlighting the combination of electrospinning with other manufacturing techniques such as microstereolithography for the creation of biodegradable rings for corneal healing<sup>16,17</sup>. In the current study the use of robocasting allows us to readily tune the design of the vascular networks in terms of size, thickness and morphology. Additionally, electrospinning allows us to create devices with different degradation speeds which can be easily scaled-up and sterilised for a future clinical application. The ability to easily spin different polymers allow us to control degradation times<sup>18</sup> and porosity opening the opportunity of developing different membrane combinations as recently reported by our group<sup>19</sup>. Specifically, electrospun mats were produced by dissolving medical grade PLGA (Purac) and PHBV (Goodfellow) in dichloromethane (DCM) and a mixture of DCM and Methanol respectively. Optimal concentrations of 20% w:w PLGA and 10% w:w of PHBV (containing 10% w:w of Methanol) were prepared and the polymers were electrospun using four 5 ml syringes with 0.6mm ID blunt tip. PLGA was spun for 1.5 hours using a rate of 30  $\mu\text{l}/\text{min}$  and, a voltage 12.5 kV and a distance between the needles and the collector of 15 cm. PHBV parameters were 1 hour of spinning, 40  $\mu\text{l}/\text{min}$  rate, a voltage of 17 kV and a distance between the needles and the collector of 17 cm. Using these parameters we obtained PLGA electrospun mats with microfibrils with diameters of  $3.5 \pm 0.5 \mu\text{m}$  and PHBV electrospun mats with nanofibrils with diameters of  $0.70 \pm 0.05 \mu\text{m}$ .

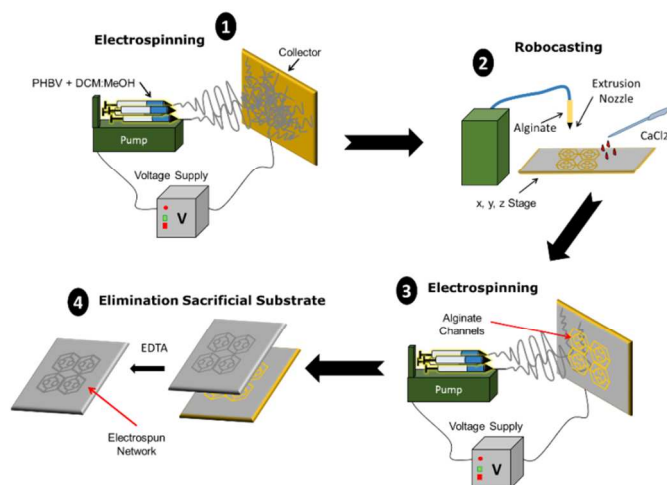


**Figure 1.** Schematic of the fabrication of synthetic vascular networks using a multi-step process. Firstly a thin layer of polymer (PHBV) is electrospun onto a flat electroplated aluminium collector. Secondly, an alginate-glycerol mixture is printed onto the electrospun sheet. Then another layer of PHBV is spun on top of the alginate pattern. Finally, alginate is removed using an ethylenediaminetetraacetic acid (EDTA) solution.

Using alginate as a sacrificial substrate in a room temperature deposition process presents several advantages: (i) the printing process can be performed without the need for a heating head; (ii) it allows introduction of biomolecules within the fabrication process so we can easily add functionality to our devices without facing loss of activity or protein denaturation and (iii) the microstructural integrity of the electrospun mats is not altered by high temperature processing. The use of other sacrificial substrates such as PVA has been also reported although in this case the extrusion cannot be done at room temperature<sup>14</sup>. Additionally, alginate is very easy to remove and is cell-friendly. The alginate paste was placed inside a syringe barrel attached to a dispensing system (Ultra 2800, EFD Inc., East Province, USA) and a 3D printer (RepRap Mendel, Oldbury on Severn, UK) was used to hold the dispensing arm and print the alginate (custom built g-code software (Vascular Pattern Path Generator, VPPG) was used to control geometry, feed-rate of the printer and the number of iterations). The alginate paste was produced by mixing 36.35g of distilled water, 0.1g of calcium chloride dihydrate (Sigma-Aldrich) 0.75g of alginic acid sodium salt (Sigma-Aldrich) and 12.125g of glycerol (Sigma-Aldrich) and it was printed using an optimum extrusion rate of 0.025cm<sup>3</sup>/min and a feed rate of 8.3 cm/s. To remove the alginate sacrificial template and achieve the creation of a hollow network between the two electrospun mats, the scaffolds were submerged in 0.5M EDTA solution overnight on a gel-shaker set to 70 rpm. Removal of the sacrificial substrate was studied by both SEM and fluorescence microscopies (Fig. 2). Eosin-Y was added to the alginate mixture and the removal process was followed using a fluorescence microscope ImageXpress system (Axon Instruments, USA). Hollow networks of sizes ranging from 0.5 mm to 2 mm were created.

For the ultimate purpose of seeding and coating the internal vascular channels with endothelial cells (ECs) a nanofibrous structure was required to prevent cell migration throughout the thickness of the scaffold.

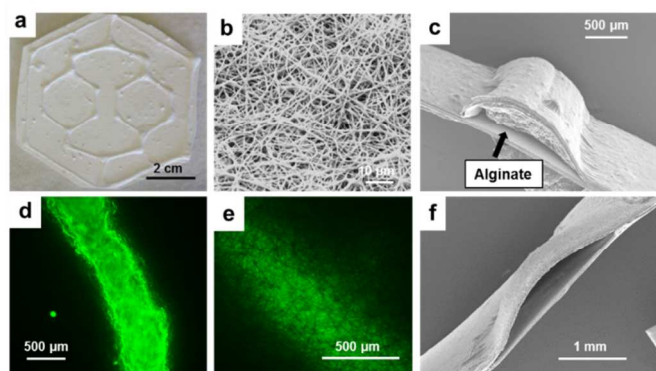


**Figure 2.** Image of PHBV artificial electrospun vascular network (a); High magnification SEM image of PHBV fibres in the vascular construct (b); SEM image of vascular conduit containing the alginate sacrificial substrate (c); Fluorescence image of alginate loaded with Eosin-Y after printing on PLGA electrospun substrate (d); Fluorescence image of alginate loaded with Eosin-Y after spinning a PLGA layer on top (e); SEM image of vascular conduit after removing the alginate sacrificial substrate (f).

Prior to cell culture mechanical properties of the PHBV scaffolds were tested and are summarised in Table 1. Briefly, tensile mechanical testing was conducted using a uniaxial load test machine fitted with a 4.5 N load cell (Bose Electroforce 3100, Bose Ltd, UK). The dimensions of strips of scaffold sheets were measured using a micrometer before being fixed to the clamps of the machine positioned 10 mm apart. Each sample was then pulled at a rate of 0.1 mm/minute and elongated to failure (n=4). Stress-strain curves were produced and the relevant values were calculated using the resultant graphs. To obtain the suture retention strength both ends of the scaffold sheet were sutured 3 mm from the end of the sample (6-0 Prolene, Ethicon Inc, USA) before being clamped in place within the uniaxial load test machine. The distance between the clamps was measured and each sample was then pulled at a rate of 0.1 mm/minute and elongated to failure (n=6). Suture retention strength was calculated as load/ (suture diameter × material thickness). The results show that the bulk material has an average ultimate tensile strength of 0.6 MPa, similar to poly(ether urethane urea) (PEUU) vascular graft scaffolds that have been used previously *in vivo*<sup>20</sup>. The suture retention strength of this material is also similar to scaffolds that have been used *in vivo* which have a typical range of between 35-59 MPa<sup>21</sup>.

After the fabrication of the constructs and the elimination of the sacrificial substrate, the scaffolds were cannulated with a 24G cannula under a dissection microscope (Wild Heerbrugg M 3Z) and their ability to be perfused was tested using a blue colour dye. The vascular nets were attached to a peristaltic pump (Watson Marlow 200 series, Scientific Laboratory Supplies, UK) via the cannula and placed into a 100 ml glass bottle containing 50 ml of media. Scaffolds were perfused at a flow rate of 0.5 ml/min for 1-5 days. Prior to cell culture, the cannulated constructs were sterilised by submerging them for 45 min in 70% ethanol (in distilled water) and then washed 3 times with sterile PBS. Initial viability and cell attachment tests were performed using HDFs (tissues were collected and used under the requirements stipulated by Research Tissue Bank Licence 12179). HDFs were cultured in DMEM supplemented with FCS (10% v/v), streptomycin (0.1 mg/ml), penicillin (100 IU/ml) and amphotericin B (0.5 g/ml) and sub-cultured as necessary. Cell viability was evaluated using the 3-(dimethylthiazol-2-yl)-2,5-diphenyltetrazolium bromide (MTT) assay and the location of the

cells on formalin-fixed constructs after 5 days of seeding was studied using Rose Bengal (1 % w:w). As expected and demonstrated in

Tensile testing (n=4)				Suture Retention Strength (MPa) (n=6)
Ultimate Tensile Strength (MPa)	Yield Strength (MPa)	Young's Modulus (MPa)	Elongation at Break (%)	
0.60 ± 0.08	0.29 ± 0.05	15.00 ± 2.60	36.47 ± 5.03	41.67 ± 5.85

Table 1 - Mechanical properties of PHBV scaffold.

previous work developed by our group cells grew and attached to both PLGA and PHBV electrospun membranes<sup>16, 17, 19, 22</sup>. The constructs were able to be perfused and following perfusion the cells were well-distributed throughout the electrospun networks. The suitability of the constructs as synthetic vascular networks was then explored using proliferating HDMECs from juvenile foreskin (Promocell, Heidelberg, Germany). Cells were grown in EC growth medium MV containing 0.05 ml/ml FCS, 0.004 ml/ml EC growth supplement, 10 ng/ml epidermal growth factor (recombinant human), 90 µg/ml heparin, 1 µg/ml hydrocortisone, 100 U/ml penicillin, 0.1 mg/ml streptomycin and 0.25 µg/ml amphotericin B. To ensure cells attached uniformly to the artificial channels we used a two-stage process. First,  $2.5 \times 10^5$  HDMECs cells (per scaffold) were seeded and kept overnight in an incubator at 37 °C and 5% CO<sub>2</sub>; the constructs were turned over the next day and a second suspension of  $2.5 \times 10^5$  HDMEC cells was seeded and left overnight. Images a-c in Figure 3 illustrate how cells attached to both the curved and the flat part of the construct. Scaffolds seeded in static conditions showed areas with irregular cell attachment indicating that perfusion was essential to achieve a more uniform distribution of cells through the electrospun network.

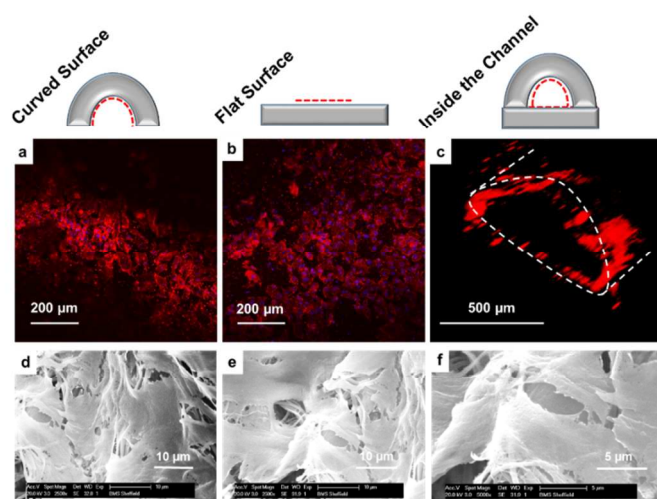


Figure 3. Fluorescence image of HDMECs cells stained with Phalloidin-TRITC (red) located on the curved surface of the artificial electrospun vascular network (a); Fluorescence image of HDMECs cells stained with Phalloidin-TRITC (red) located on the flat surface of the artificial electrospun vascular network (b); Confocal z-stack of the vascular construct showing an homogenous distribution of cells (red) throughout the artificial construct (c); SEM images of HDMECs cells attached to the PHBV constructs (d-f).

Delivering cells of endothelial origin has been the focus of many studies aimed at enhancing neovascularization as they are directly associated with contributing to vessel formation. However, improved results have been noted by using a co-culture of ECs and so called 'helper cells'. Studies using HDMECs and HDFs have shown improved cell proliferation and cell signalling<sup>23</sup> and it is believed that this is as a result of paracrine signalling mechanisms that promote production of VEGF from fibroblasts and the up-regulation of VEGF receptors on HDMECs<sup>24</sup>. In an attempt to improve the surface coverage of HDMECs throughout the vascular channels, HDFs were co-cultured within this system. Briefly HDMECs were seeded using the same quantities and two staged process described above, but in these experiments  $2.5 \times 10^5$  HDFs suspended in EC growth medium MV containing 0.05 ml/ml FCS, 0.004 ml/ml EC growth supplement, 10 ng/ml epidermal growth factor (recombinant human), 90 µg/ml heparin, 1 µg/ml hydrocortisone, 100 U/ml penicillin, 0.1 mg/ml streptomycin and 0.25 µg/ml amphotericin B, were seeded onto both outer surfaces of the scaffold and cultured for 5 days. Samples were prepared and imaged for SEM using methods described previously<sup>17</sup>. Immunohistochemistry was also performed by fixing the samples in 3.7% formalin for 3 hours and then freezing in OCT media (Tissue-Tek, Fisher Scientific, UK). Samples were then sectioned into 20µm slices using a cryostat (Leica CM1100). Slides were submerged three times in PBS to remove the OCT media before being incubated with 7.5% (w/v) bovine serum albumin (BSA) (Sigma Aldrich) at room temperature for 1 hour. Samples were then incubated overnight at 4°C with mouse monoclonal anti-human CD31 (1:20 in 1% (w/v) BSA) (Dako, UK). The scaffold sections were incubated with Alexa Fluor® 633nm goat anti-mouse secondary antibody (1:200, Life Technologies) for 1 hour at room temperature before washing and finally counterstaining with nuclear stain DAPI. Figure 4 clearly shows the improved HDMEC cell coverage within the channels when using a co-culture of HDMECs and HDFs (d-f) when compared to HDMECs alone (a-c). With co-culture there appeared to be a continuous layer of CD31 positive cells within the channels. In the absence of HDFs this layer was not continuous.

We have developed a technique for the fabrication of bespoke constructs with applications in the regeneration of vascular tissues. We have demonstrated that HDMECs attach uniformly to our constructs when co-cultured with HDFs and that we can easily tune our scaffolds in terms of chemical nature, size and morphology. Furthermore, the constructs can be made of a range of polymers with different rates of degradation. It is important to highlight the final design of our constructs which are made of a flat bottom and a curved upper surface (Figs. 2c, 2f, 3a-c). Other authors have reported vascular networks with a fully cylindrical structure e.g. Morgan et al.<sup>11</sup> reported on the creation of rounded vessels using collagen. Further

development of the 4-Step protocol we present in this study will allow us to create round channels in the future.

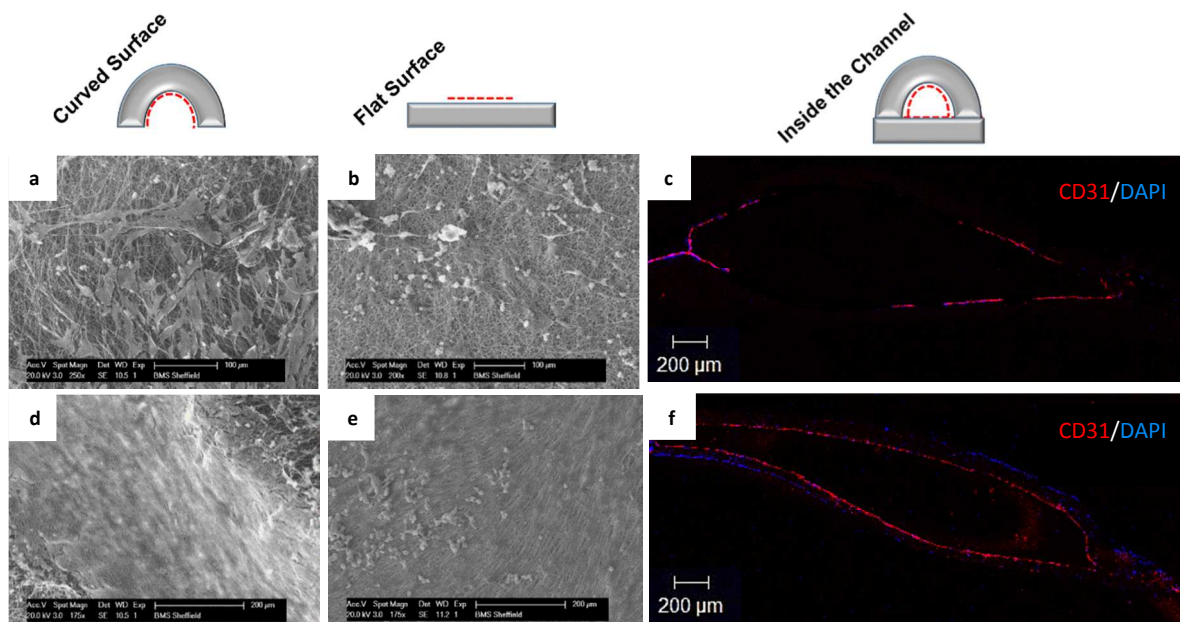


Figure 4 – SEM images of curved and flat surfaces of vascular channels showing sporadic coverage of HDMECs when these were added on their own (a-b); Fluorescence image showing CD31 positive cells (red) with DAPI counterstaining (blue) throughout a cross section of the scaffold when HDMECs were cultured alone confirming the irregular cell coverage (c); SEM images of curved and flat surfaces of vascular channels showing a uniform sheet like coverage of HDMECs when a co-culture of HDMECs within the channels and HDFs on the outer surfaces of the scaffold were used (d-e); A representative fluorescence image indicating the uniform coverage within a cross section of the scaffold using a co-culture of HDMECs and HDFs (f).

## Conclusions

In summary the aim of this work is to report a reproducible and robust way of fabricating scaffolds which can be used as models for studying vascular regeneration and may ultimately be part of a biomaterial device to assist in neovascularisation of tissue engineered tissues. There are many factors which are thought to contribute to neovascularisation *in vivo* – cell combinations, pro-angiogenic signals and the influence of blood flow - which makes this a difficult area of study as this complexity cannot be readily reproduced in *in vitro* studies. We suggest this simple vascular network will prove a useful model system to advance our knowledge of neovascularisation as we will be able to study the combination of these factors in a controlled environment. Thus future work will include the use of varying cell combinations in conjunction with perfusion bioreactors to more closely reproduce the *in vivo* environment. Furthermore, the scaffolds can also be functionalised using molecules such as heparin which in turn will bind specific angiogenic factors like Vascular Endothelial Growth Factor (VEGF) using methods recently developed by our group based on flexible layer-by-layer coating strategies<sup>25</sup>.

## Acknowledgments

We thank EPSRC Landscape Fellowship and the DTC Tissue Engineering Regenerative Medicine programs for funding this research. Special thanks go to Dr Sabiniano Roman for his help with the mechanical testing of the scaffolds.

## Notes and references

a Bioengineering and Health Technologies Group, The School of Clinical Dentistry, University of Sheffield, Sheffield, UK.

b Biomaterials and Tissue Engineering Group, Department of Materials Science and Engineering, Kroto Research Institute, University of Sheffield, Sheffield, UK.

\* Corresponding Authors: Dr. Iñida Ortega Asencio (Email: [I.ortega@sheffield.ac.uk](mailto:I.ortega@sheffield.ac.uk), Tel: +44(0)1142265543) & Dr. Frederik Claeyssens (Email: [f.claeyssens@sheffield.ac.uk](mailto:f.claeyssens@sheffield.ac.uk), Tel: +44 (0) 114 222 5513)

# These authors have contributed equally to this work.

1. F. A. Auger, L. Gibot and D. Lacroix, *Annual review of biomedical engineering*, 2013, **15**, 177-200.
2. L. H. Nguyen, N. Annabi, M. Nikkha, H. Bae, L. Binan, S. Park, Y. Kang, Y. Yang and A. Khademhosseini, *Tissue engineering. Part B, Reviews*, 2012, **18**, 363-382.
3. H. C. Ko, B. K. Milthorpe and C. D. McFarland, *European cells & materials*, 2007, **14**, 1-18; discussion 18-19.
4. S. Ravi and E. L. Chaikof, *Regenerative medicine*, 2010, **5**, 107-120.
5. B. S. Conklin, E. R. Richter, K. L. Kreutziger, D. S. Zhong and C. Chen, *Medical Engineering & Physics*, 2002, **24**, 173-183.
6. P. J. Schaner, N. D. Martin, T. N. Tulenko, I. M. Shapiro, N. A. Tarola, R. F. Leichter, R. A. Carabasi and P. J. DiMuzio, *Journal of Vascular Surgery*, 2004, **40**, 146-153.
7. L. Gui, A. Muto, S. A. Chan, C. K. Breuer and L. E. Niklason, *Tissue engineering. Part A*, 2009, **15**, 2665-2676.
8. L. Mancuso, A. Gualerzi, F. Boschetti, F. Loy and G. Cao, *Biomedical materials (Bristol, England)*, 2014, **9**, 045011.
9. H. C. Ott, T. S. Matthiesen, S.-K. Goh, L. D. Black, S. M. Kren, T. I. Netoff and D. A. Taylor, *Nat Med*, 2008, **14**, 213-221.
10. B. E. Uygun, A. Soto-Gutierrez, H. Yagi, M. L. Izamis, M. A. Guzzardi, C. Shulman, J. Milwid, N. Kobayashi, A. Tilles, F. Berthiaume, M. Hertl, Y. Nahmias, M. L. Yarmush and K. Uygun, *Nat Med*, 2010, **16**, 814-820.

11. J. P. Morgan, P. F. Delnero, Y. Zheng, S. S. Verbridge, J. Chen, M. Craven, N. W. Choi, A. Diaz-Santana, P. Kermani, B. Hempstead, J. A. López, T. N. Corso, C. Fischbach and A. D. Stroock, *Nat. Protocols*, 2013, **8**, 1820-1836.
12. J. S. Miller, K. R. Stevens, M. T. Yang, B. M. Baker, D.-H. T. Nguyen, D. M. Cohen, E. Toro, A. A. Chen, P. A. Galie, X. Yu, R. Chaturvedi, S. N. Bhatia and C. S. Chen, *Nat Mater*, 2012, **11**, 768-774.
13. M. Centola, A. Rainer, C. Spadaccio, S. De Porcellinis, J. A. Genovese and M. Trombetta, *Biofabrication*, 2010, **2**, 014102.
14. E. M. Jeffries, S. Nakamura, K.-W. Lee, J. Clampfner, H. Ijima and Y. Wang, *Macromolecular Bioscience*, 2014, n/a-n/a.
15. B. Duan, L. A. Hockaday, K. H. Kang and J. T. Butcher, *Journal of biomedical materials research. Part A*, 2013, **101**, 1255-1264.
16. I. Ortega, A. J. Ryan, P. Deshpande, S. MacNeil and F. Claeysens, *Acta Biomater*, 2013, **9**, 5511-5520.
17. I. Ortega, R. McKean, A. J. Ryan, S. MacNeil and F. Claeysens, *Biomaterials Science*, 2014.
18. K. A. Blackwood, R. McKean, I. Canton, C. O. Freeman, K. L. Franklin, D. Cole, I. Brook, P. Farthing, S. Rimmer, J. W. Haycock, A. J. Ryan and S. MacNeil, *Biomaterials*, 2008, **29**, 3091-3104.
19. F. J. Bye, J. Bissoli, L. Black, A. J. Bullock, S. Puwanun, K. Moharamzadeh, G. C. Reilly, A. J. Ryan and S. MacNeil, *Biomaterials Science*, 2013, **1**, 942-951.
20. W. He, A. Nieponice, L. Soletti, Y. Hong, B. Gharaibeh, M. Crisan, A. Usas, B. Peault, J. Huard, W. R. Wagner and D. A. Vorp, *Biomaterials*, 2010, **31**, 8235-8244.
21. Y. Hong, K. Takanari, N. J. Amoroso, R. Hashizume, E. P. Brennan-Pierce, J. M. Freund, S. F. Badylak and W. R. Wagner, *Tissue Engineering Part C: Methods*, 2011, **18**, 122-132.
22. F. J. Bye, L. Wang, A. J. Bullock, K. A. Blackwood, A. J. Ryan and S. MacNeil, 2012, e4172.
23. K. R. Stevens, K. L. Kreutziger, S. K. Dupras, F. S. Korte, M. Regnier, V. Muskheli, M. B. Nourse, K. Bendixen, H. Reinecke and C. E. Murry, *Proceedings of the National Academy of Sciences*, 2009, **106**, 16568-16573.
24. H. Li and J. Chang, *Acta Biomaterialia*, 2013, **9**, 6981-6991.
25. C. D. Easton, A. J. Bullock, G. Gigliobianco, S. L. McArthur and S. MacNeil, *Journal of Materials Chemistry B*, 2014, **2**, 5558-5568.